ENGINEERING JOURNAL

Article

Model Reference Input Shaping Using Quantitative Feedforward-Feedback Controller

Withit Chatlatanagulchai

Control of Robot and Vibration Laboratory, Department of Mechanical Engineering, Faculty of Engineering, Kasetsart University, 50 Ngam Wong Wan Rd, Lat Yao, Chatuchak, Bangkok 10900, Thailand
E-mail: fengwtc@ku.ac.th

Abstract. Input shaping convolutes the reference signal with a sequence of impulses, whose amplitudes and timings are designed to produce a shaped reference that avoids exciting lightly-damped modes to reduce residual vibration from a quick movement. The input shaper can be made robust to uncertain mode parameters by adding more impulses, which delays the reference signal, resulting in longer move time. Instead of using more impulses, in this paper, a feedforward-feedback control system, based on the quantitative feedback theory, is placed in the loop to match the closed-loop system, with uncertain plant, to a known reference model. The feedforward-feedback system handles the uncertainty, so the input shaper, placed outside the loop, needs not be robust. The closed-loop system emphasizes on selected frequencies and reduces the cost of feedback. It is shown that the proposed feedforward-feedback system is less conservative than the pure-feedback system. Other sources of vibration such as external disturbances and noise can be handled by the feedforward-feedback system as well. Simulation shows that the proposed technique can withstand large plant uncertainty with fast move time when compared to traditional robust input shaper.

Keywords: Vibration, quantitative feedback, input shaping, model reference, command shaping, robust input shaper.

1. Introduction

The input shaper is viewed as a filter that reduces the vibrations induced by external sources such as reference input, disturbances, and noise. Since vibration reduction is not the only objective of the control system, the input shaper is often implemented together with feedback controller.

In general, there are two configurations; either the input shaper is placed outside or inside the feedback loop. Although placing the input shaper inside the loop can reduce vibrations from all external sources, there are some limitations for the design of the feedback controller due to additional time delay introduced by the input shaper. Meanwhile, placing the input shaper outside the loop only reduces vibration from the reference input but without additional limitations.

Several researchers have investigated placing the input shaper outside the loop together with different types of feedback controller: iterative learning controller by Zolfagharian *et al.* in [1]; genetic algorithm by Aldebrez *et al.* in [2]; sliding mode controller by Pai in [3] and by Hu *et al.* in [4]; PD controller by Huey and Singhose in [5] and by Kenison and Singhose in [6]; and adaptive controller by Dharne and Jayasuriya in [7]. A feedback controller based on quantitative feedback theory (QFT) is used in this paper.

QFT was introduced by Horowitz in [8] as a loop shaping control design technique that extends the work of Bode in [9]. It is so-called quantitative because various specifications such as tracking, disturbances and noise rejections, relative stability, and model matching are graphically displayed on the Nichols chart for the designer to make trade-off among them. At a specific frequency, instead of being viewed as a point on the Nichols chart, the plant is now viewed as a template, which is an area containing possible plant values due to uncertainties. The loop shaping process results in a feedback controller and a prefilter that ensure the closed-loop system meet all specifications for all uncertain plants. Model matching capability of the QFT is what emphasized in this paper.

Several researchers have used feedback control system to match the closed-loop system to a reference model. The input shaper is then designed using vibratory mode parameters of the reference model. Pai in [10] used ADALINE neural network to enforce both sliding and reaching phases in a sliding mode control to make model matching error go to zero despite parameter variations and external disturbance. Only simulation was presented, and the complexity and global convergence of this time-domain algorithm may pose implementation problem. Other closely related works to [10] that used sliding mode controller for reference model matching are [11]-[16]. Yu and Chang in [17] used a PI controller to match the closed-loop system of a piezoelectric nano-positioner to a reference model, while Yu and Chang in [18] used a P controller to match the closed-loop system of a dual solenoid actuator to a reference model. Both works used zero-vibration input shaper. However, the design of the PI or P controller was heuristic; and there was no mention about attainable specifications or allowable uncertainty. Dharne and Jayasuriya in [7] used a direct model reference adaptive control to match the closed-loop system to a reference model. The technique may therefore be susceptible to insufficiently persistent excitation of input, global instability, and divergence of adapted parameters.

In this paper, instead of using signal-based reference model matching as in other previous works, system-based method is considered. Closeness between the reference model and the closed-loop system from reference input to output is formulated as a frequency-domain specification. The plant is allowed to be uncertain. This uncertainty together with the specification can be converted to bounds on the Nichols chart. A proposed feedforward-feedback controller, which is shown to be less conservative than the pure-feedback controller, is designed to loop-shape the open-loop system to satisfy all bounds. Simulation on a benchmark mass-damper-spring plant, with 35% uncertainties in all plant parameters, shows that the closed-loop system matches the reference model well within the pre-specified specification. A zero-vibration (ZV) input shaper is placed outside the loop and is designed from the vibratory mode parameters of the reference model. The responses to step reference inputs, for all uncertain plants, show significant vibration reduction using the proposed system compared to using the open-loop ZV and robust input shapers. Vibrations induced by disturbances and noise are also reduced by the system.

The materials and methods section contains the following content. First are details of robust input shaping. Details include finding amplitudes and time locations of the impulses in the input shaper, how robust input shaper is obtained, and how to apply the input shaper as an open-loop system. Second is the proposed model reference input shaping system, consisting of a ZV input shaper and a feedforward-feedback quantitative controller. In this section, model matching bounds are derived for both feedforward-feedback and pure-feedback cases. The results section contains a simulation on a benchmark mass-damper-spring plant.

The control design steps are demonstrated, followed by the simulation results. The results section is followed by discussion and conclusion sections.

2. Materials and Methods

2.1. Robust Input Shaping

Input shaping was originated by Singer and Seering in [19] based on the Posicast control of Smith in [20] and Tallman and Smith in [21]. Excellent review of the input shaping technique can be found in [22].

The technique includes finding amplitudes and time locations of the impulses in an impulse train by solving: 1) residual vibration constraint; 2) robustness constraint; 3) impulse amplitude constraint; and 4) time optimality constraint. The resulting impulse train is then convoluted with the reference input resulting in a shaped reference input that 1) avoids exciting the system vibratory modes for minimal residual vibration; 2) is robust against vibratory mode parameter variations; 3) has the same final value as that of the original reference input; and 4) arrives at the final value in the shortest time.

To formulate the residual vibration constraint, consider a unit, single-impulse response of a one DOF, lightly-damped system, after an applied time t_1, given by

$$y_1(t) = \frac{e^{-\zeta \omega_n (t-t_1)}}{m \omega_n \sqrt{1-\zeta^2}} \sin \sqrt{1-\zeta^2} \omega_n (t-t_1),$$

where y_1 is the response, ω_n is the natural frequency, ζ is damping ratio, and m is mass. The amplitude of the sine function at the applied time $t = t_1$ is given by

$$A_\uparrow = \frac{1}{m \omega_n \sqrt{1-\zeta^2}}.$$

Next, consider an n-impulses response, after the applied time of the nth impulse, t_n, given by

$$y_\Sigma(t) = \sum_{i=1}^{n} \frac{A_i e^{-\zeta \omega_n (t-t_i)}}{m \omega_n \sqrt{1-\zeta^2}} \sin \sqrt{1-\zeta^2} \omega_n (t-t_i),$$

where A_i is the ith impulse magnitude and t_i is the applied time of the ith impulse. Using a trigonometric identity, the sum of n impulse responses at $t = t_n$ is given by

$$A_\Sigma = \frac{1}{m \omega_n \sqrt{1-\zeta^2}} e^{-\zeta \omega_n t_n} \sqrt{\left[C(\omega_n, \zeta) \right]^2 + \left[S(\omega_n, \zeta) \right]^2},$$

where C and S are given by

$$C(\omega_n, \zeta) = \sum_{i=1}^{n} A_i e^{\zeta \omega_n t_i} \cos\left(\omega_n \sqrt{1-\zeta^2} t_i \right),$$

$$S(\omega_n, \zeta) = \sum_{i=1}^{n} A_i e^{\zeta \omega_n t_i} \sin\left(\omega_n \sqrt{1-\zeta^2} t_i \right).$$

The ratio between A_Σ and $A_\uparrow$ is a non-dimensional quantity so-called *percentage vibration*, which gives the ratio of vibration with input shaping to that without input shaping. The residual vibration constraint is then given by

$$V(\omega_n, \zeta) = \frac{A_\Sigma}{A_\uparrow} = e^{-\zeta \omega_n t_n} \sqrt{\left[C(\omega_n, \zeta) \right]^2 + \left[S(\omega_n, \zeta) \right]^2} = V_{tol}, \tag{1}$$

where V_{tol} is a desired percentage of vibration, normally set to zero.

The robustness constraint is found from setting derivatives of $V(\omega_n, \zeta)$, with respect to its variables, to zero, as given by

$$\frac{\partial V(\omega_n, \zeta)}{\partial \omega_n} = 0 \text{ or } \frac{\partial V(\omega_n, \zeta)}{\partial \zeta} = 0. \tag{2}$$

This constraint reduces the sensitivity of the percentage vibration to uncertainties in ω_n and ζ.

The impulse amplitude constraint is simply a requirement, given by

$$\sum_{i=1}^{n} A_i = 1, \tag{3}$$

to ensure that the shaped reference input has the same final value as that of the original reference input.

Because the residual vibration constraint contains sine and cosine terms, there will be infinite number of solutions. The time optimality constraint is simply to find the shortest t_n, as given by

$$\min(t_n). \tag{4}$$

By solving constraints (1), (3), and (4), and setting $V_{tol} = 0$, one obtains a so-called *zero vibration (ZV)* input shaping with two impulses whose magnitudes and time locations are given by

$$\begin{bmatrix} A_i \\ t_i \end{bmatrix} = \begin{bmatrix} \dfrac{1}{1+K} & \dfrac{K}{1+K} \\ 0 & \dfrac{\pi}{\omega_n\sqrt{1-\zeta^2}} \end{bmatrix}, \tag{5}$$

where K is given by

$$K = e^{\frac{-\zeta\pi}{\sqrt{1-\zeta^2}}}.$$

In addition, if the robustness constraint (2) is also included, one obtains a so-called *zero vibration derivative (ZVD)* input shaping with three impulses whose magnitudes and time locations are given by

$$\begin{bmatrix} A_i \\ t_i \end{bmatrix} = \begin{bmatrix} \dfrac{1}{1+2K+K^2} & \dfrac{K}{1+2K+K^2} & \dfrac{K^2}{1+2K+K^2} \\ 0 & \dfrac{\pi}{\omega_n\sqrt{1-\zeta^2}} & \dfrac{2\pi}{\omega_n\sqrt{1-\zeta^2}} \end{bmatrix}. \tag{6}$$

If the robustness constraint also includes second-order derivatives onward, the resulting input shapers will be with four or more impulses and are so-called *ZVDD, ZVDDD,* and so on. More impulses means more robustness but with longer time to the final reference value.

Because of their simplicity, the ZV and ZVD input shapers will be compared with the proposed technique in this paper. Other robust input shaping techniques are the extra-insensitive (EI) by Singhose *et al.* in [23] and the specified-insensitivity (SI) by Singer and Seering in [24]. In EI, multi-humped vibration sensitivity curve, which is the plot of the percentage vibration versus natural frequency variation, is first specified. Then, the robustness constraint (2) is replaced by constraints on the desired percentage vibration and the zero slopes at the top of the humps. In SI, the residual vibration constraint (1) becomes a set of constraints, each for a specified frequency. A specified V_{tol} is applied across the specified frequency range. It was shown that both EI and SI techniques are less sensitive to parameter variation than the family of the ZVD technique when the same shaper duration is considered. However, they are more complicated.

Figure 1 shows the input shaper applied to an uncertain plant, where $\bar{r}$ is the original reference input, r is the shaped reference input, and y is the output.
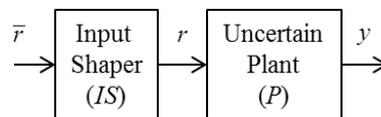

Fig. 1.   Application of the input shaper to an uncertain plant.

2.2. Model Reference Input Shaping with Quantitative Feedback Controller

Even though the robust input shapers, such as the ZVD, can handle uncertainties in parameter variations, they come at a price of having longer time to reach final reference set-point. From (6), the shaped reference input of the ZVD reaches its final value at $t_2 = 2\pi / \left[\omega_n\sqrt{1-\zeta^2} \right]$, which is twice that of the ZV.

For shorter move time, in this section, we investigate using feedback control system together with the non-robust ZV input shaper. The job of handling the parameter uncertainties is delegated to the feedback control system. The input shaper is placed outside of the loop to reduce vibration induced by reference input, while the feedback system makes the uncertain closed-loop system match a reference model and reduces vibration induced by disturbances and noise. Two types of quantitative control systems, which use pure feedback and feedforward-feedback, are considered.

Consider a closed-loop system in Fig. 2, whose, in addition to those in Fig. 1, e, d_I, u, d_O, and n are tracking error, plant-input disturbance, control input, plant-output disturbance, and noise, respectively. The quantitative feedback control system consists of a feedback controller G and a prefilter F. They will be designed so that the mapping from r to y matches a reference model M, given by

$$\left| M - \frac{Y}{R} \right| = \left| M - \frac{PGF}{(1+PG)} \right| < \delta_m,$$

where δ_m is a small number that determines how close the uncertain closed-loop system be to the exact reference model. Compared to that in Fig. 1, the quantitative feedback control system G and F helps the input shaper in handling the uncertainty from the plant.
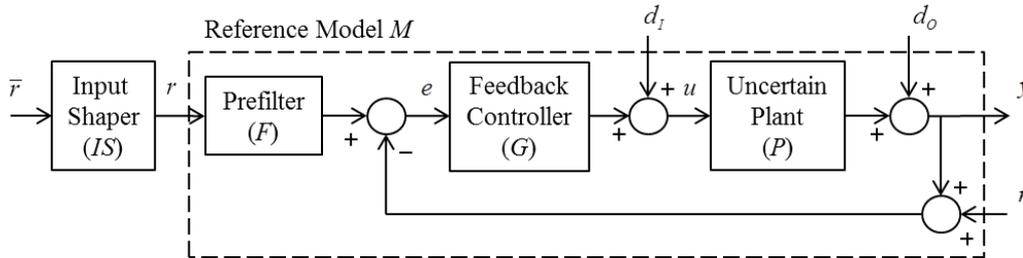

Fig. 2.   Model reference input shaping with quantitative feedback controller.

When $F = M$ and $M = P_0$, where P_0 is the nominal plant, the frequency-domain specification above becomes that given by

$$\left| \frac{P_0}{1+PG} \right| < \delta_m. \tag{7}$$

Further derivation leads to $\left| G + 1/P \right| > \delta_m^{-1} \left| P_0 / P \right|$, which shows that, on the complex plane, G must be shaped so that $\left| G + 1/P \right|$ is greater than $\delta_m^{-1} \left| P_0 / P \right|$ as shown in Fig. 3.
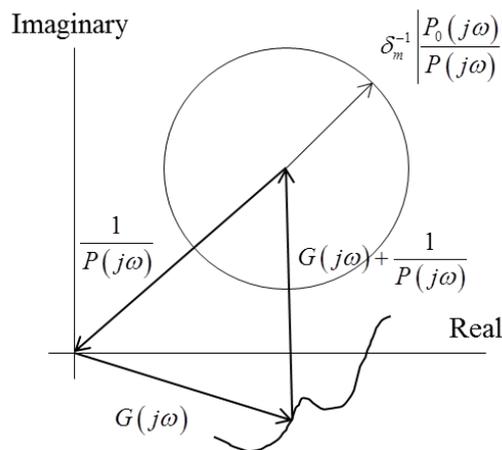

Fig. 3.   Allowable region for $G(j\omega)$.

2.3. Model Reference Input Shaping with Quantitative Feedforward-Feedback Controller

In this section, we investigate using feedforward together with feedback controllers. The underlying principle is simply to use feedforward with what we know and to use feedback with what we do not. Information on nominal plant and measured disturbances and noise can be used to design feedforward controller. The feedback contribution can be reduced resulting in lower cost of feedback.

Consider a closed-loop system in Fig. 4 with a feedforward controller G_r. For matching with the reference model M, the frequency-domain specification is given by

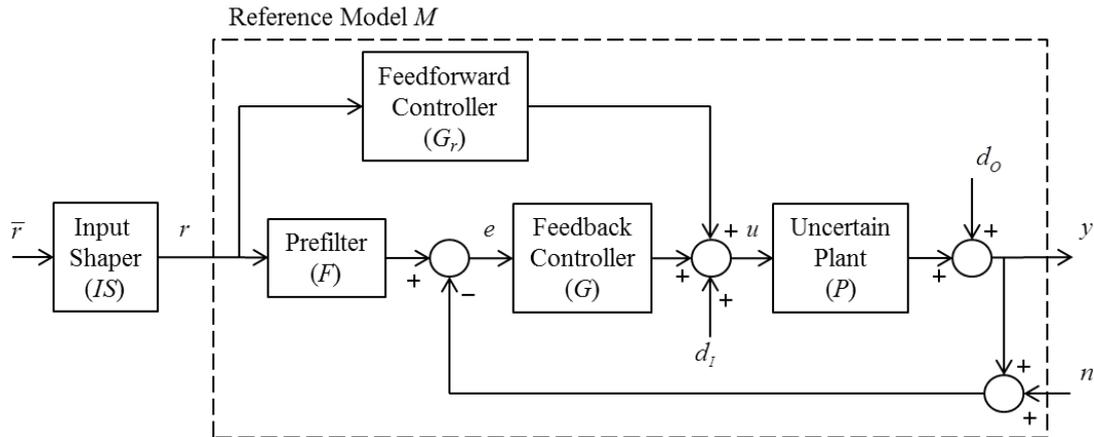$$\left| M - \frac{Y}{R} \right| = \left| M - \frac{PG_r + PGF}{1+PG} \right| < \delta_m, \tag{8}$$

Fig. 4.   Model reference input shaping with quantitative feedforward-feedback controller.

When $F = M$, $M = P_0$, and $G_r = M / P_0$, the specification above becomes that given by

$$\left| \frac{P_0 - P}{1 + PG} \right| < \delta_m. \tag{9}$$

Comparing (9) to (7), we now have $\left| G + 1/P \right| > \delta_m^{-1} \left| (P_0 - P)/P \right|$, which shows that, for frequencies where the uncertain plant does not deviate from the nominal plant much, we will have larger allowable region for $G(j\omega)$, that is, the specification (9) is then less conservative than (7).

3.   Results

In this section, the simulation results on implementing the proposed technique to a benchmark mass-damper-spring are presented.

3.1.   Simulation Example

An *m-c-k* benchmark problem, shown in Fig. 5, will be used as the uncertain plant to compare the system in Fig. 4 to those in Fig. 1 and Fig. 2. This benchmark problem was used by Cole and Wongratanaphisan in [25]. The transfer function from x_1 to x_2 is given by

$$\frac{X_2}{X_1} = \frac{cs + k}{ms^2 + cs + k},$$

whose nominal parameter values are $m = 1$ kg, $k = 1.5791 \times 10^4$ kg.s^{-2}, and $c = 25.1327$ kg.s^{-1}, corresponding to a natural frequency $\omega_n = 40\pi$ rad.s^{-1} and a damping ratio $\zeta = 0.1$.
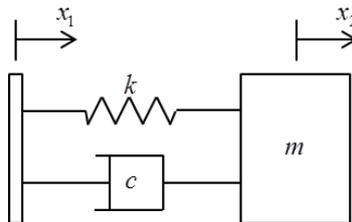
Fig. 5.   A benchmark m-c-k system.

Assume 35% uncertainties in each parameter, that is, $m \in \{0.65, 1.35\}$, $c \in \{16.336, 33.929\}$, and $k \in \{1.0264, 2.1318\} \times 10^4$, and select working frequencies $\omega = \{10, 50, 100, 120, 150, 200, 500\}$ rad.s^{-1}, which sufficiently cover low, high, as well as the natural frequency of the system. The control system will be designed with specifications (7) and (9) for all uncertain plants in the uncertain regions.

For the feedback system in Fig. 2, the specification (7) with $G = 1$ and $\delta_m = -20\,\text{dB} = 0.1$ is converted to bounds on the Nichols chart as shown in Fig. 6(Top). Each bound represents boundary of the allowable region, shown in Fig. 3, for $L_0 = GP_0$, for all plant uncertainties and for a specified frequency. Fig. 6(Top) also contains the original shape of $L_0 = GP_0$. To be in the allowable region, L_0 must be shaped to be above or outside its bounds for all working frequencies.

Figure 6(Middle) contains the shaped L_0. Because the plant is of type 0, to obtain zero step input tracking, we first appended an integrator $1/s$. Then a real zero $(s/7.661 + 1)$ was added to increase the overall phase of the system. A constant gain of 234.4 was then added to shift the shape up above its bounds. Note that we deliberately violated the bounds at 120 and 150 rad.s^{-1} to avoid too high gains around the natural frequency. Finally, a complex pole $1/(s^2/3439^2 + 2(0.565)s/3439 + 1)$ was added to have higher roll-off rate at high frequencies beyond 1000 rad.s^{-1} to avoid high-frequency noise. The overall feedback controller becomes that given by

$$G = \frac{234.4}{s}\left(\frac{s}{7.661}+1\right)\left(\frac{1}{\dfrac{s^2}{3439^2}+\dfrac{2(0.565)s}{3439}+1}\right). \tag{10}$$

For the feedforward-feedback system in Fig. 4, as mentioned before, the specification (9) is less conservative than (7) especially for frequencies where the uncertain plant does not deviate from the nominal plant much. With $\delta_m = -20\,\text{dB} = 0.1$, they were converted to bounds on the Nichols chart as shown in Fig. 6(Bottom). The bounds for all frequencies, except those for 100 and 120 rad.s^{-1}, are lower than those bounds of the feedback-only system, resulting in a less conservative controller G with lower constant gain of 166.7, while other components of G stay the same. Frequencies 100 and 120 rad.s^{-1} are where the uncertain plant does deviate from the nominal plant the most.

Figure 7 contains Bode magnitude plots of the feedback controller (10) (in solid line) and feedforward-feedback controller (in dashed line). The feedforward-feedback controller is less conservative and therefore has less cost of feedback than the feedback-only controller.

Figure 8 only shows the Bode magnitude plots in the feedforward-feedback case. Figure 8(Above) displays the plots of the reference model $M = P_0$ in dashed line and of the closed-loop transfer functions $Y/R = (PG_r + PGF)/(1 + PG)$ in multiple solid lines. Each solid line represents the transfer function computed from each uncertain plant in the set. The feedback controller G, the prefilter F, and the feedforward controller G_r were designed to make the mapping Y/R match the reference model M according to the specification (8) for working frequencies ranging from 10 to 500 rad.s^{-1}. Figure 8(Below) shows the plots of the reference model $M = P_0$ in dashed line and of the plant P in multiple solid lines. It can be seen that without the closed-loop system, the uncertain plant can differ much from its nominal value. Since the input shaper was designed from the reference model $M = P_0$, the deviation should adversely affect its performance in reducing the residual vibration as will be seen next.

Several time-domain tracking results are presented in Fig. 9 using a sampling period of 0.001 second. The ZV input shaper is given by (5) and the ZVD input shaper is given by (6). Both were designed from the natural frequency ω_n and the damping ratio ζ of the nominal plant P_0. The model reference input shaping with quantitative feedback control system in Fig. 2 uses the ZV input shaper, the controller G given by (10), and the prefilter $F = P_0$. The model reference input shaping with quantitative feedforward-feedback control system in Fig. 4 uses the ZV input shaper, the controller G given by (10) but with the constant gain 166.7, the prefilter $F = P_0$, and the feedforward controller $G_r = 1$.

Figure 9(a) contains the output x_2 from all uncertain plants for the feedforward-feedback system in Fig. 4. Figure 9(b) is for the feedback system in Fig. 2. The shaped reference input from the ZV input shaper is in dashed line. Both systems deliver good tracking result with almost no overshoot and with short settling time. However, the feedforward-feedback system can reach the steady-state setpoint faster because the feedforward term uses the known nominal plant and therefore can act faster than the feedback term.

Figures 9(c) and (d) contain the output x_2 for the open-loop system in Fig. 1. Figure 9(c) is when the ZV input shaper is used, and Fig. 9(d) is when the ZVD input shaper is used. Without the closed-loop system, the outputs from the uncertain plants oscillate heavily even when the robust ZVD input shaper is used.

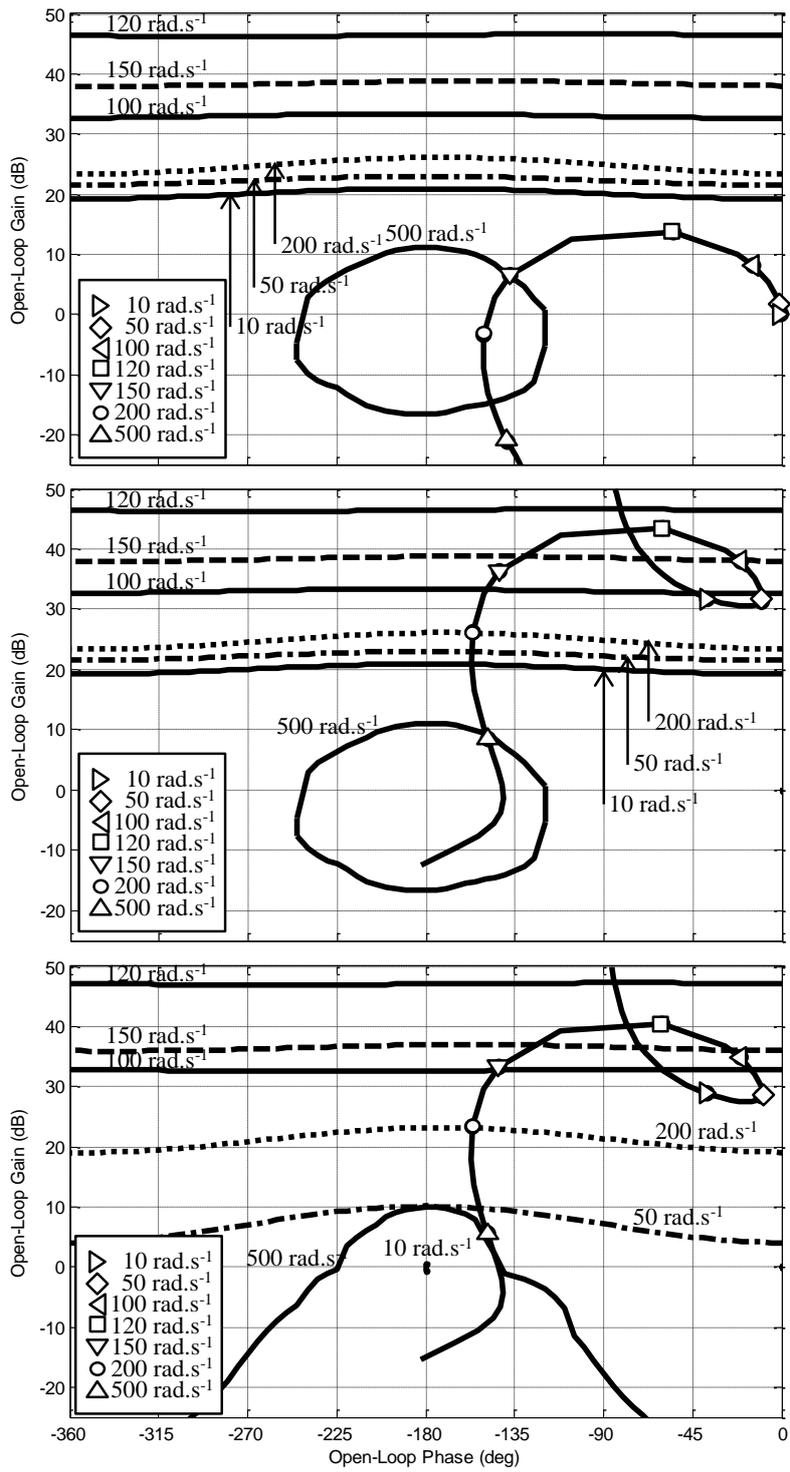Fig. 6.   Loop shaping for the m-c-k system. (Top) Unshaped. (Middle) Feedback. (Bottom) Feedforward-feedback.
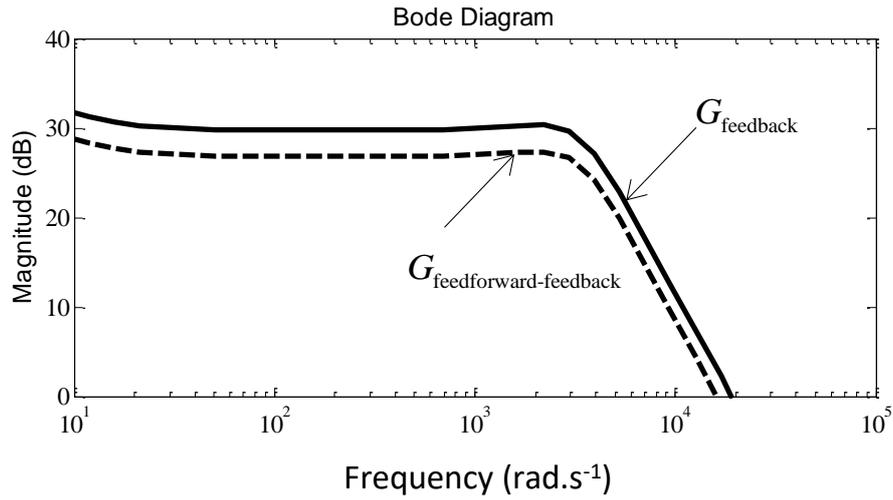
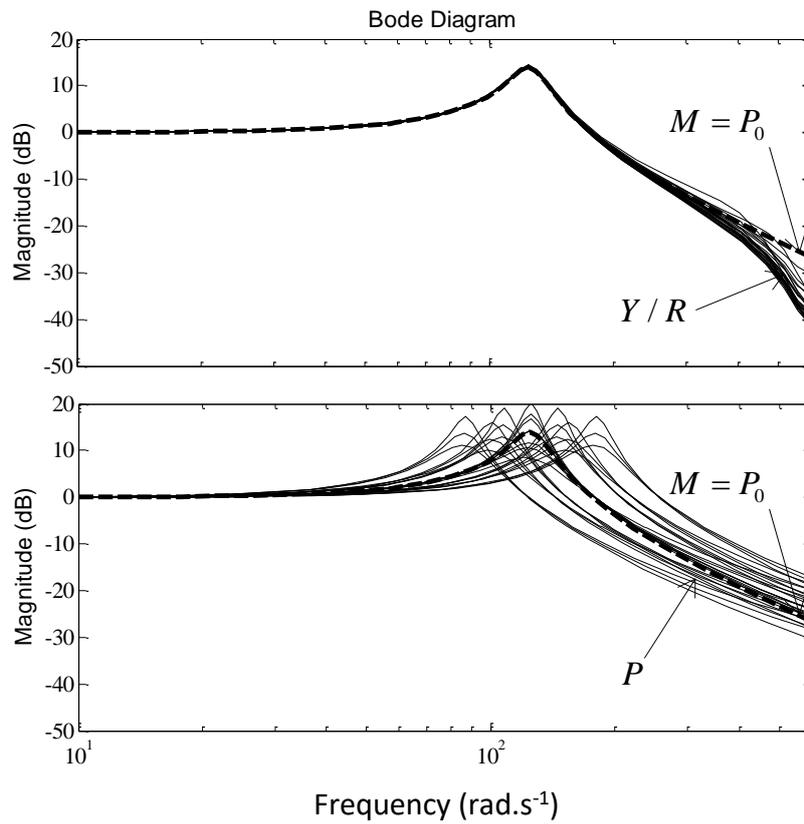Fig. 7.   Bode magnitude plots of the feedback and feedforward-feedback controllers.

Fig. 8.   Bode plots in the feedforward-feedback case. (Above) The reference model M in dashed line and the mapping Y / R. (Below) The reference model M in dashed line and the uncertain plant P.
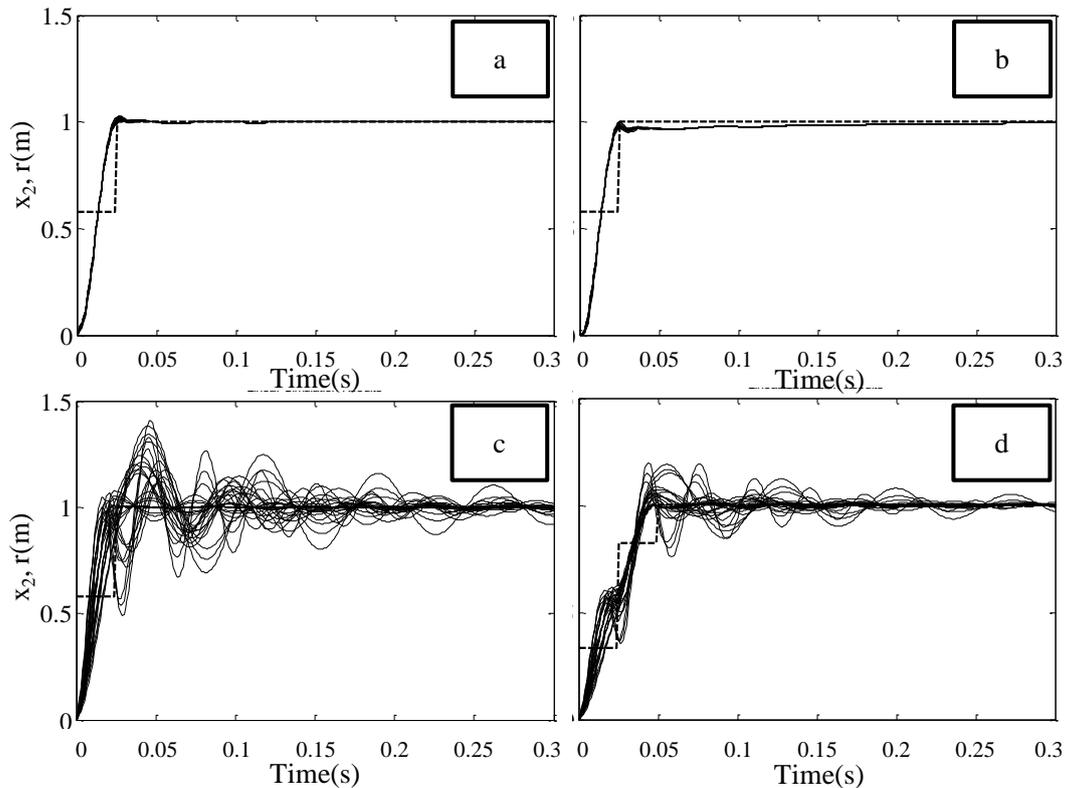
Fig. 9. Tracking of the output x_2: (a) for the feedforward-feedback system with ZV input shaper, (b) for the feedback system with ZV input shaper, (c) for the open-loop system with ZV input shaper, and (d) for the open-loop system with ZVD input shaper.

3.2. Reduction of Vibration Induced by Disturbances and Noise

Vibration can also come from disturbances and noise. The input shaper, placed outside of the loop, cannot reduce these vibrations. In this section, we demonstrate that the feedback controller in Fig. 2 and Fig. 4 can be designed to reject disturbances and noise to suppress these vibrations.

From Fig. 4, we can include the following frequency-domain specifications in the quantitative feedback system design:

1) Plant-output disturbance rejection, as given by

$$\left|y/d_O\right| = \left|1/(1+PG)\right| < \delta_{dO},$$

2) Plant-input disturbance rejection, as given by

$$\left|y/d_I\right| = \left|P/(1+PG)\right| < \delta_{dI},$$

3) Noise rejection, as given by

$$\left|y/n\right| = \left|PG/(1+PG)\right| < \delta_n,$$

where δ_{dO}, δ_{dI}, and δ_n are small positive numbers. Each specification is converted to bounds on the Nichols chart for the open-loop shaping process. We will not design a new control system here but will apply the same control system as in the previous section to demonstrate the ability to reduce vibrations induced by disturbances and noise.

Figures 10(a) to 10(b) show the output x_2, from the open-loop system in Fig. 1, when there exist unit-step plant-output disturbance or unit-step noise, respectively. Fig. 10(c) to Fig. 10(d) are the results from the feedforward-feedback system in Fig. 4. By comparing Fig. 10(a) to Fig. 10(c) and Fig. 10(b) to Fig. 10(d), we can see that the feedforward-feedback system can also reduce vibrations induced by disturbance and noise by attenuating their influences on the output.
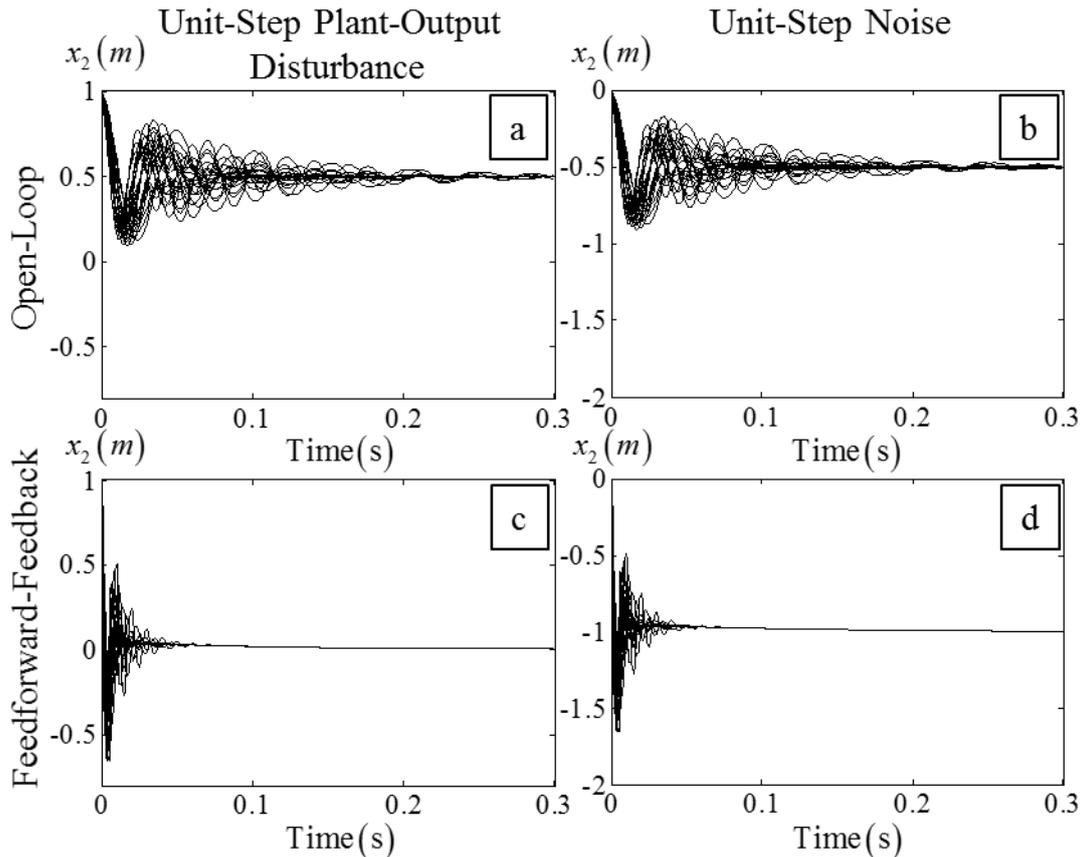
Fig. 10. Output from disturbance and noise: (a)-(b) with open-loop system, (c)-(d) with feedforward-feedback system.

3.3. Summary of the Design Process

The design process can be summarized in the following steps:
1) Obtain the nominal plant model, P_0.
2) Choose a reference model, for example, $M = P_0$.
3) Specify uncertain sets of model parameters that the control system will tolerate, for example, $m \in \{0.65, 1.35\}$.
4) Select working frequencies, ω.
5) Plot plant templates on the Nichols chart to inspect the boundaries of the uncertain plant for each working frequency.
6) Specify model matching specifications, (7) or (9).
7) Specify other specifications such as stability margin, tracking, noise rejection, disturbance rejection.
8) Plot the original open-loop shape on the Nichols chart, that is, L_0.
9) Obtain the controller, G, by performing open-loop shaping on the Nichols chart by appending transfer functions, for example, integrator, lead/lag to have the final shape lie in the allowable regions.
10) Choose the pre-filter as $F = M$ and choose the feedforward controller as $G_r = M / P_0$.
11) Obtain simulation result in the frequency domain and confirm that all specifications are met.
12) Design an input shaper from the reference model, M.
13) Obtain simulation result in the time domain.
14) Apply the control system to a hardware.

Figure 11 contains a flow chart summarizing the design process.

```
┌─────────────────────────────────┐
│    Obtain nominal plant model   │
└─────────────────────────────────┘
                 ↓
┌─────────────────────────────────┐
│     Choose a reference model    │
└─────────────────────────────────┘
                 ↓
┌─────────────────────────────────┐
│      Specify uncertain sets     │
└─────────────────────────────────┘
                 ↓
┌─────────────────────────────────┐
│    Select working frequencies   │
└─────────────────────────────────┘
                 ↓
┌─────────────────────────────────┐
│  Plot plant templates on the Nichols chart  │
└─────────────────────────────────┘
                 ↓
┌─────────────────────────────────┐
│ Specify model matching specification │
└─────────────────────────────────┘
                 ↓
┌─────────────────────────────────┐
│    Specify other specifications │
└─────────────────────────────────┘
                 ↓
┌─────────────────────────────────┐
│ Plot the original open-loop shape on the Nichols chart │
└─────────────────────────────────┘
                 ↓
┌─────────────────────────────────┐
│ Obtain the controller, G, by performing open-loop shaping │
└─────────────────────────────────┘
                 ↓
┌─────────────────────────────────┐
│ Choose the pre-filter and the feedforward controller │
└─────────────────────────────────┘
                 ↓
┌─────────────────────────────────┐
│ Obtain simulation result in the frequency domain │
└─────────────────────────────────┘
                 ↓
┌─────────────────────────────────┐
│       Design an input shaper    │
└─────────────────────────────────┘
                 ↓
┌─────────────────────────────────┐
│ Obtain simulation result in the time domain │
└─────────────────────────────────┘
                 ↓
┌─────────────────────────────────┐
│ Apply the control system to a hardware │
└─────────────────────────────────┘
```

Fig. 11. Flow chart of the design process.

4. Discussion

From Fig. 7, the proposed feedforward-feedback system has lower gain than the pure feedback system while still delivers equally good performance. This lower gain reduces the control effort used as well as avoids more noise at high frequencies. The reason for this improvement is that the feedforward term, which represents the known part of the uncertain plant, helps reduce the amount of feedback needed; therefore, the cost of feedback is reduced.

From Fig. 8, using the proposed feedforward-feedback system in the model reference setting results in small deviation of the closed-loop system from the reference model. Figure 8 also shows large deviation of the uncertain plant from the reference model without using the proposed system. The input shaper is designed using the natural frequencies and damping ratios of the reference model. As a result, with the proposed system, the input shaper needs not be robust and can have shorter duration for faster movement.

From Fig. 9, it can be seen that the tracking performance using the proposed feedforward-feedback system is slightly better than that of the pure feedback system, which is a result of using feedforward term. Nevertheless, both systems substantially outperform the ZV and ZVD input shapers by having more robustness to model uncertainty and smaller settling time.

From Fig. 10, it is obvious that the open-loop input shaping cannot handle vibrations induced by external disturbance and noise. The proposed feedforward-feedback system utilizes feedback to reduce vibrations induced by disturbance and noise while maintains good robustness to plant model uncertainty.
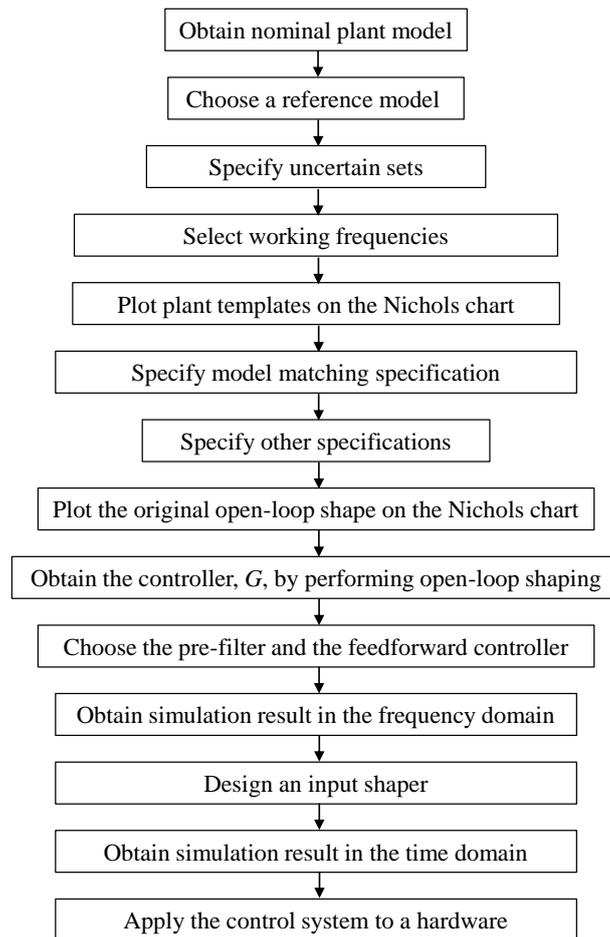
5. Conclusion

Two very practical techniques are fused together in this paper. Input shaper reduces vibration from reference input, while quantitative feedforward-feedback controller reduces vibrations from disturbances and noise.

The quantitative controller is also designed to match the closed-loop system to a reference model, whose vibratory mode parameters are used in the design of the input shaper. The quantitative controller explicitly takes into account the amount of the plant uncertainty and various achievable frequency-domain specifications during the design process.

Model matching enhances robustness of the input shaper to plant model uncertainty, without increasing the number of impulse and move time. The quantitative controller can be designed such that the resulting closed-loop system, which matches the reference model, has less and specifiable uncertainty than that of the original uncertain plant.

The proposed technique of using the input shaper and the quantitative controller is simple yet practical enough to be applied to complicated as well as nonlinear plants. For these plants, we need to find a central linear plant model and be sure its uncertain region or plant template covers all possible plants in all operating points. Gain scheduling may be used to obtain multiple linear plant models. This can reduce the size of the uncertain region, resulting in tighter specifications.

The proposed technique can be naturally extended to multi-mode systems by including the multi modes in the reference model. Extension to multi-input-multi-output (MIMO) systems can be more challenging because the quantitative controller may only be suitable for diagonal plant. H_∞-based controller, for model matching, may be more suitable to the MIMO systems.

Acknowledgments

References

[1] A. Zolfagharian, A. Noshadi, M. Z. M. Zain, and A. R. A. Bakar, "Practical multi-objective controller for preventing noise and vibration in an automobile wiper system," *Swarm and Evolutionary Computation*, vol. 8, pp. 54-68, February 2013.

[2] F. M. Aldebrez, M. S. Alam, and M. O. Tokhi, "Input-shaping with GA-tuned PID for target tracking and vibration reduction," in *Mediterranean Conference on Control and Automation*, Limassol, Cyprus, 2005, pp. 485-490.

[3] M.-C. Pai, "Robust input shaping control for multi-mode flexible structures using neuro-sliding mode output feedback control," *Journal of the Franklin Institute*, vol. 349, pp. 1283-1303, April 2012.

[4] Q. Hu, X. Z. Gao, and G. Ma, "Reference model variable structure output feedback for attitude maneuvers control of flexible spacecrafts," *Intelligent Automation and Soft Computing*, vol. 15, pp. 53-62, 2009.

[5] J. R. Huey and W. Singhose, "Design of proportional-derivative feedback and input shaping for control of inertia plants," *IET Control Theory and Applications*, vol. 6, pp. 357-364, February 2012.

[6] M. Kenison and W. Singhose, "Concurrent design of input shaping and proportional plus derivative feedback control," *Journal of Dynamic Systems, Measurement, and Control*, vol. 124, pp. 398-405, July 2002.

[7] A. G. Dharne and S. Jayasuriya, "Increasing the robustness of the input-shaping method using adaptive control," in *American Control Conference*, Denver, Colorado, 2003, pp. 1578-1583.

[8] I. Horowitz, "Fundamental theory of linear feedback control systems," *Trans. IRE on Auto. Control*, vol. 4, pp. 5-19, 1959.

[9] H. W. Bode, *Network Analysis and Feedback Amplifier Design*. New York, NY: Van Nostrand, 1945.

[10] M.-C. Pai, "Robust input shaping control for multi-mode flexible structures using neuro-sliding mode output feedback control," *Journal of the Franklin Institute*, vol. 349, pp. 1283-1303, April 2012.

[11] M.-C. Pai, "Robust input shaping control for multi-mode flexible structures," *International Journal of Control, Automation, and Systems*, vol. 9, pp. 23-31, 2011.

[12] M.-C. Pai and A. Sinha, "Increasing robustness of input shaping method to parametric uncertainties and time-delays," *Journal of Dynamic Systems, Measurement, and Control*, vol. 133, 2011.

[13] M.-C. Pai, "Closed-loop input shaping control of vibration in flexible structures using discrete-time sliding mode," *International Journal of Robust and Nonlinear Control*, vol. 21, pp. 725-737, 2011.

[14] Q.-L. Hu, Z. Wang, and H. Gao, "Sliding mode and shaped input vibration control flexible systems," *IEEE Transactions on Aerospace and Electronic Systems*, vol. 44, pp. 503-519, 2008.

[15] Q. Hu, "Robust integral variable structure controller and pulse-width pulse-frequency modulated input shaper design for flexible spacecraft with mismatched uncertainty/disturbance," *ISA Transactions*, vol. 46, pp. 505-518, October 2007.

[16] Q. Hu and G. Ma, "Maneuvers and vibration suppression of flexible spacecraft integrating variable structure control and input shaping technique," *Trans. Japan Soc. Aero. Space Sci.*, vol. 48, pp. 205-212, 2006.

[17] L. Yu and T. N. Chang, "Model reference zero vibration control of ultrahigh precision piezoelectric nanopositioner," in *American Control Conference*, Baltimore, MD, 2010, pp. 5856-5861.

[18] L. Yu and T. N. Chang, "Variable model reference high precision position control of dual solenoid actuator," in *Annual Conference of IEEE Industrial Electronics*, Orlando, FL, 2008, pp. 2609-2614.

[19] N. C. Singer and W. C. Seering, "Preshaping command inputs to reduce system vibration," *ASME J. of Dynamics System, Measurement and Control*, vol. 112, pp. 76-82, March 1990.

[20] O. J. M. Smith, "Posicast control of damped oscillatory systems," in *Proceedings of the IRE*, September 1957, vol. 45, pp. 1249-1255.

[21] G. H. Tallman and O. J. M. Smith, "Analog study of dead-beat posicast control," *IRE Transactions on Automatic Control*, pp. 14-21, March 1958.

[22] W. Singhose, "Command shaping for flexible systems: A review of the first 50 years," *International Journal of Precision Engineering and Manufacturing*, vol. 10, pp. 153-168, October 2009.

[23] W. E. Singhose, W. P. Seering, and N. C. Singer, "Shaping inputs to reduce vibration: A vector diagram approach," in *1990 IEEE Int. Conf. on Robotics and Automation*, Cincinnati, OH, 1990, pp. 922-927.

[24] N. C. Singer and W. P. Seering, "An extension of command shaping methods for controlling residual vibration using frequency sampling," in *1992 IEEE International Conference on Robotics and Automation*, Nice, France, 1992, pp. 800-805.

[25] M. O. T. Cole and T. Wongratanaphisan, "A direct method of adaptive FIR input shaping for motion control with zero residual vibration," *IEEE/ASME Transactions on Mechatronics*, vol. 18, pp. 316-327, 2013.